

Electronic Supporting Information

Self-Exfoliation of 2D Covalent Organic Frameworks: Morphology Transformation Induced by Solvent Polarity

Na Zhang^a, Taisheng Wang^a, Xing Wu^a, Chen Jiang^a, Fang Chen^a, Wei Bai^{b*}, and Ruke Bai^{a*}

^a CAS Key Laboratory of Soft Matter Chemistry, Department of Polymer Science and Engineering, University of Science and Technology of China, Hefei 230026, P. R. China

^b Department of Chemistry, University of Tennessee, Knoxville, TN 37996, United States.

Tel 86-551-63600722; Fax 86-551-63631760

^aE-mail: bairk@ustc.edu.cn

^bE-mail: baiwei81@gmail.com

Table of Contents

1. Instruments and Methods.

Figure S1. Synthetic route of the **A2**, **B3** and **C2**.

Figure S2. FT-IR spectra of **A2**, **B3**, **C2**, **iCOFs-A** and **COFs-B**.

Table S1. Peak assignments for FT-IR spectrum of **iCOFs-A**

Table S2. Peak assignments for FT-IR spectrum of **COFs-B**

Figure S3. Solid-state ¹³C-CP/MAS NMR spectroscopies of **A2**, **B3**, **C2**, **iCOFs-A** and **COFs-B**.

Figure S4. Element analysis of **iCOFs-A**.

Figure S5. Thermogravimetric analysis (TGA) of **iCOFs-A** and **iCONs-A**.

Figure S6. Experimental PXRD patterns of **COFs-B**.

Figure S7. Pore size distribution of **COFs-B** and Nitrogen sorption isotherms for **COFs-B** at 77 K.

Figure S8. AFM images and height profiles of nanospheres (a) and nanosheets (b,c) transformed from **iCOFs-A**.

Figure S9. SEM (a,b,c) and TEM (d,e,f) images of **COFs-B** in different solvents.

Figure S10. SEM images of the uniform **iCONs-A** thin films on silicon substrate (a,b), which showed the re-accumulated nanosheets; I–V profile of **iCONs-A** (red curve: without light irradiation; blue curve: upon light irradiation) (c); PXRD patterns of **iCONs-A** thin films on silicon substrate (d).

Figure S11. TEM images of **iCOFs-A** in various organic solvents.

Figure S12-S25. NMR Data

Figure S26. Synthetic route of the model compound.

1. Instruments and Methods.

Transmission electron microscopy (TEM)

Transmission electron microscopy was performed on a Philips CM 200/FEG transmission electron microscope. The samples were prepared by carefully dropping the corresponding solution onto the carbon coated copper grid followed by removal of the solvent under vacuum.

Atomic force microscopy (AFM)

Atomic force microscopy was carried out with a Nano scope IIIa MultiMode microscope. The samples were prepared by drop-casting of the corresponding solution (diluted with distilled water) on mica or silicon wafers, dried under air for 2 h, and then submitted to AFM characterization.

Fourier-transform infrared spectroscopy (FT-IR)

Fourier transform infrared spectroscopy was carried out with a Nicolet 380 FT-IR spectrometer. The samples for IR study were prepared as KBr pellets.

Thermal properties

Thermogravimetric analysis (TGA) was performed on a TGA 851 (Mettler Toledo) from room temperature to 600 °C at the heating rate of 10 °C min⁻¹ under N₂.

Powder X-ray diffraction

X-ray diffraction measurements were carried out with an X'Pert PROX system using monochromated Cu/K α ($\lambda = 0.15418$ nm). The samples were spread on the square recess of XRD sample holder as a thin layer, respectively.

Photoelectricity measurements

Electrical conductivity and photoconductivity measurements of the **iCONS-A** were carried out through a two-probe method using an Agilent B1500A Precision semiconductor parameter analyzer coupled a Signatone S-1160 probe station, which is equipped with a Motic microscope and a CCD camera for in situ imaging of the device. The whole system is housed in a shielding dark box to eliminate the noise and/or scattering light for low-current and/or light-sensitive measurements. The micro-gap electrodes were fabricated by photolithography silicon wafer covered with a 300 nm thick SiO₂ dielectric layer. The gold electrode pair is 50 μ m long and 5 μ m wide, onto which nanosheets were deposited by drop-casting, followed by air-drying. We investigated the photoconductivity of **iCONS-A** by casting a thin film of **iCONS-A** on gold electrode with the irradiation from visible light (>400 nm) of

a xenon lamp.

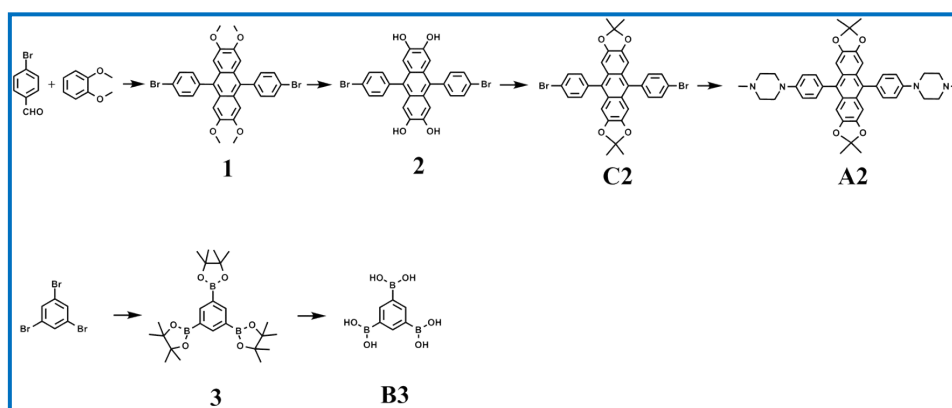


Figure S1. Synthetic route of the A2, B3 and C2.

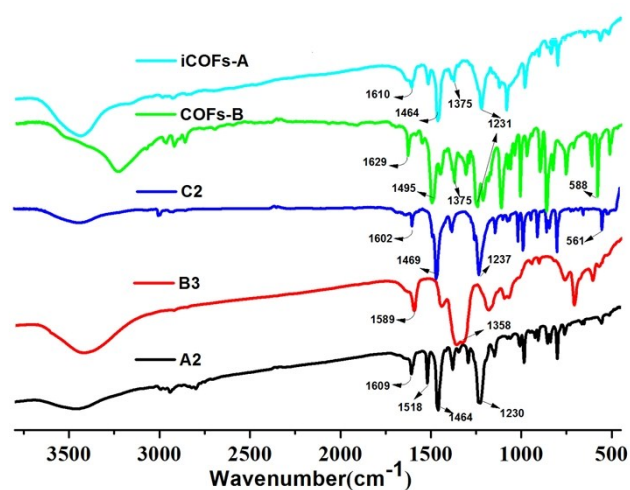


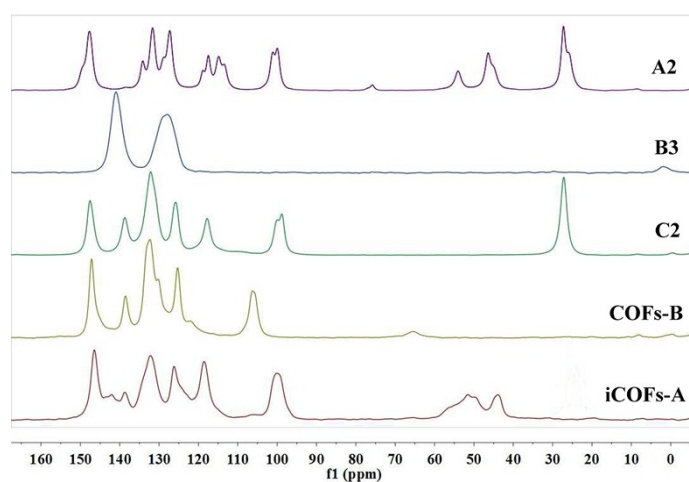
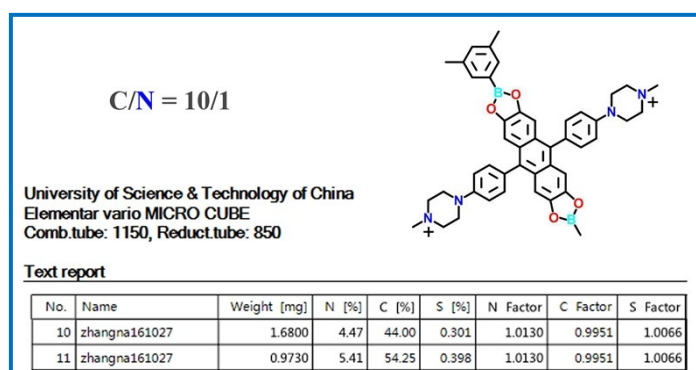
Figure S2. FT-IR spectra of A2, B3, C2, iCOFs-A and COFs-B.

Table S1. Peak assignments for FT-IR spectrum of iCOFs-A

Peak (cm ⁻¹)	Assignment and Notes
3437 (m)	H ₂ O
2935 (w)	C-H stretching
2846 (w)	
1610(w) C=C	stretch in typical region for fused aromatics
1522(w) C=C	stretch in typical region for fused aromatics
1464 (m)	C-N ⁺ stretch
1375 (m)	B-O stretch, characteristic band for borate ester
1231 (m)	C-O stretch, characteristic band for borate ester
1132 (w)	C-H in plane bending modes.
1087 (m)	

Table S2. Peak assignments for FT-IR spectrum of COFs-B

Peak (cm ⁻¹)	Assignment and Notes
3232	H ₂ O
1629 C=C 1495	stretch in typical region for fused aromatics
C=C	stretch in typical region for fused aromatics
1375	B–O stretch, characteristic band for borate ester
1231	C–O stretch, characteristic band for borate ester
1120	C–H in plane bending modes.
1010	
588	C–Br stretch

**Figure S3.** Solid-state ¹³C-CP/MAS NMR spectroscopies of A2, B3, C2, iCOFs-A and COFs-B.**Figure S4.** Element analysis of iCOFs-A.

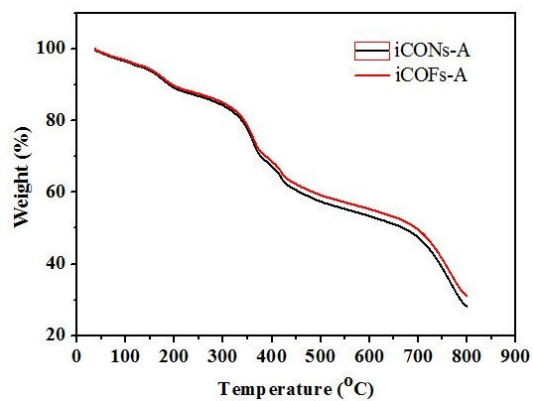


Figure S5. Thermogravimetric analysis (TGA) of **iCOFs-A** and **iCONs-A**. Both of the TGA profiles of **iCONs-A** and **iCOFs-A** showed a initial stage of thermal weight loss below 200 °C which was attributed to the evaporation of water absorbed by ionic groups on the **iCONs-A**.

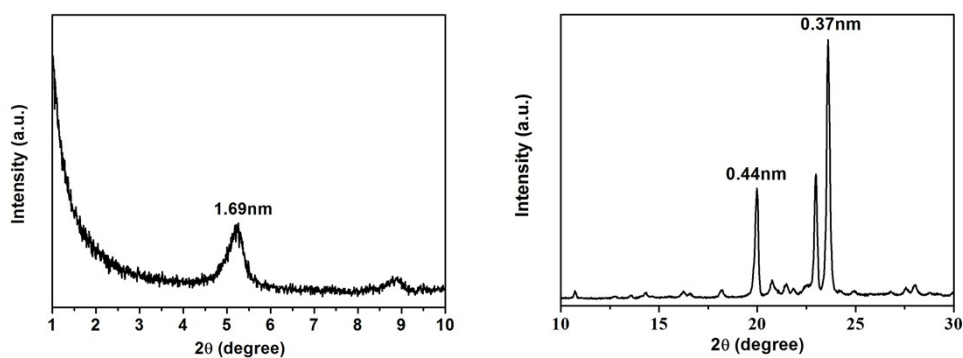


Figure S6. Experimental PXRD patterns of **COFs-B**.

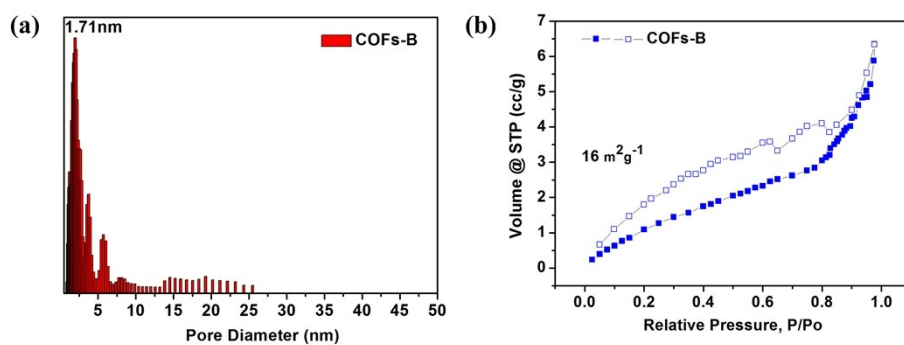


Figure S7. Pore size distribution of **COFs-B** and Nitrogen sorption isotherms for **COFs-B** at 77 K.

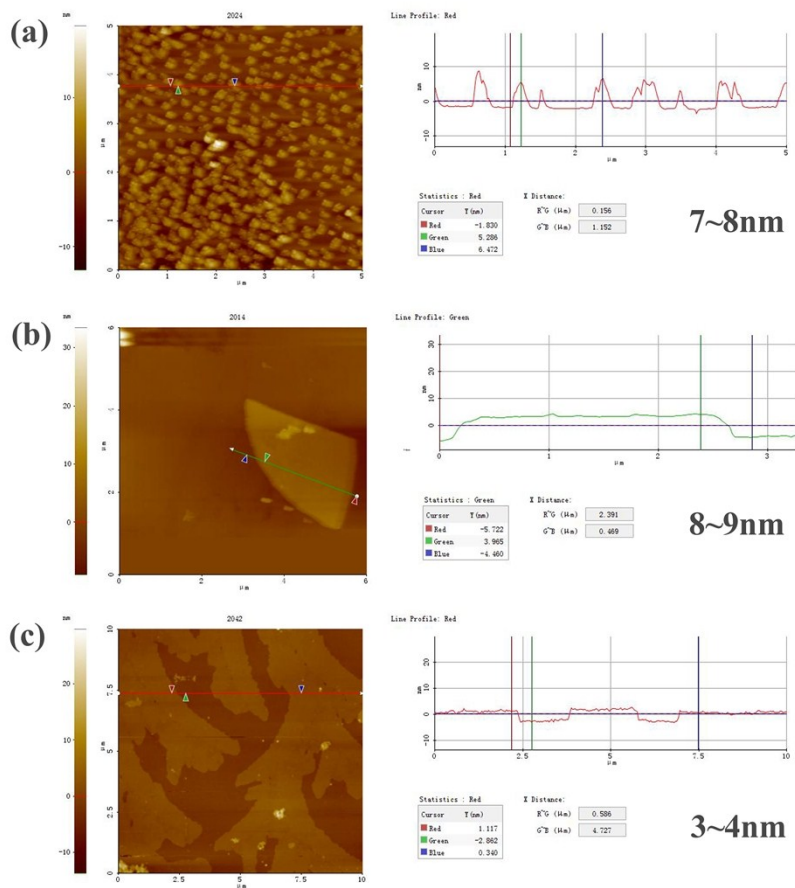


Figure S8. AFM images and height profiles of nanospheres (a) and nanosheets (b,c) transformed from iCOFs-A.

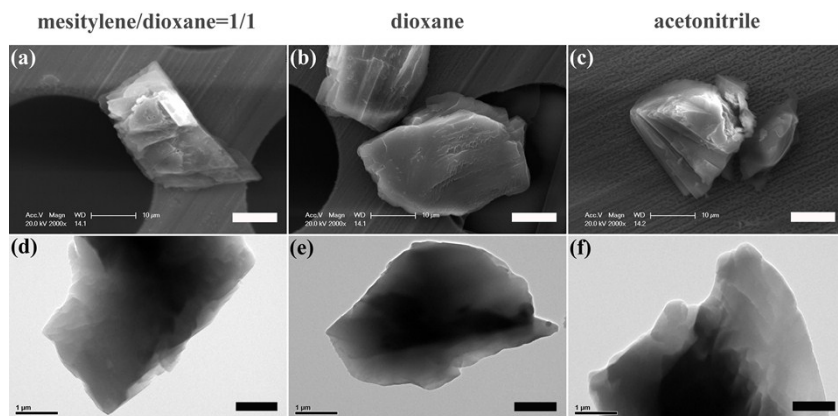


Figure S9. SEM (a,b,c) and TEM (d,e,f) images of COFs-B in different solvents. Scale bars: a) 10 μm , b) 10 μm , c) 10 μm , d) 1 μm , e) 1 μm , f) 1 μm .

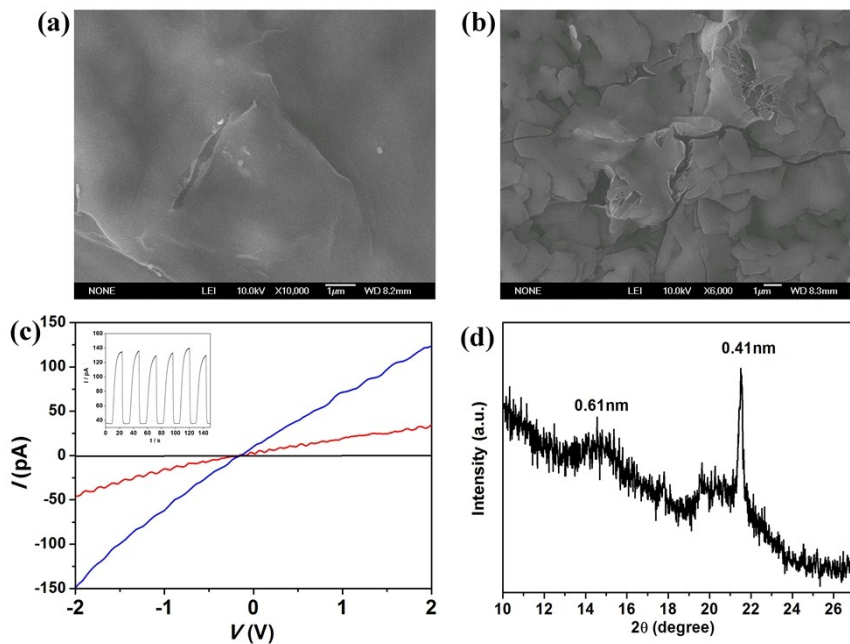


Figure S10. SEM images of the uniform iCONs-A thin films on silicon substrate (a, b), which showed the re-accumulated nanosheets; I–V profile of iCONs-A (red curve: without light irradiation; blue curve: upon light irradiation) (c) (Insert: Photocurrent when the light was turned on or off.); PXRD patterns of iCONs-A thin films on silicon substrate(d).

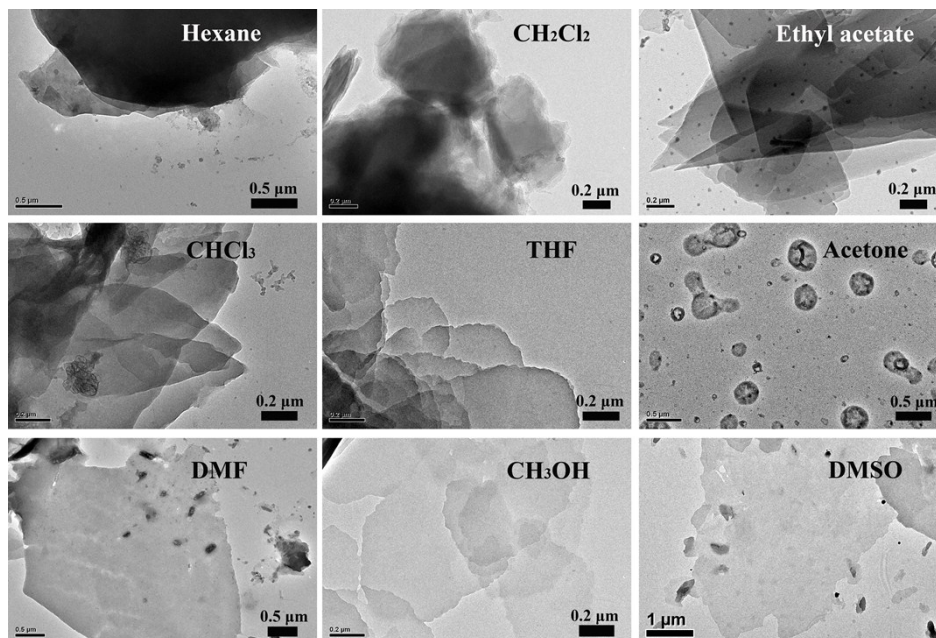


Figure S11. TEM images of iCOFs-A in various organic solvents.

NMR Data

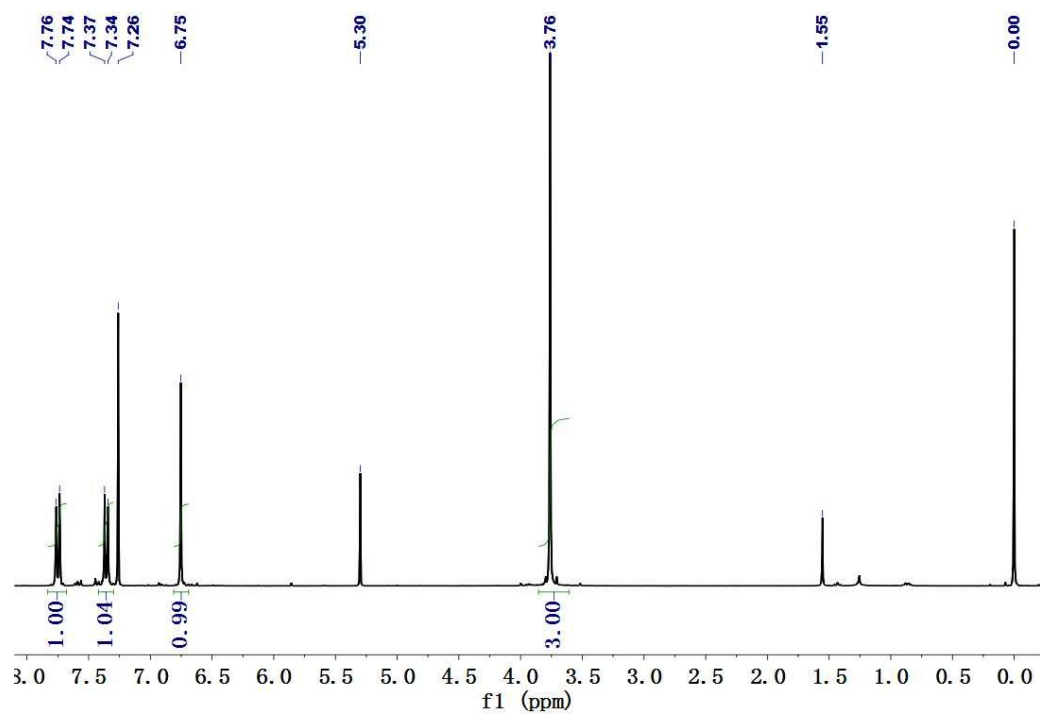


Figure S12. ¹H NMR spectrum of compound 1.

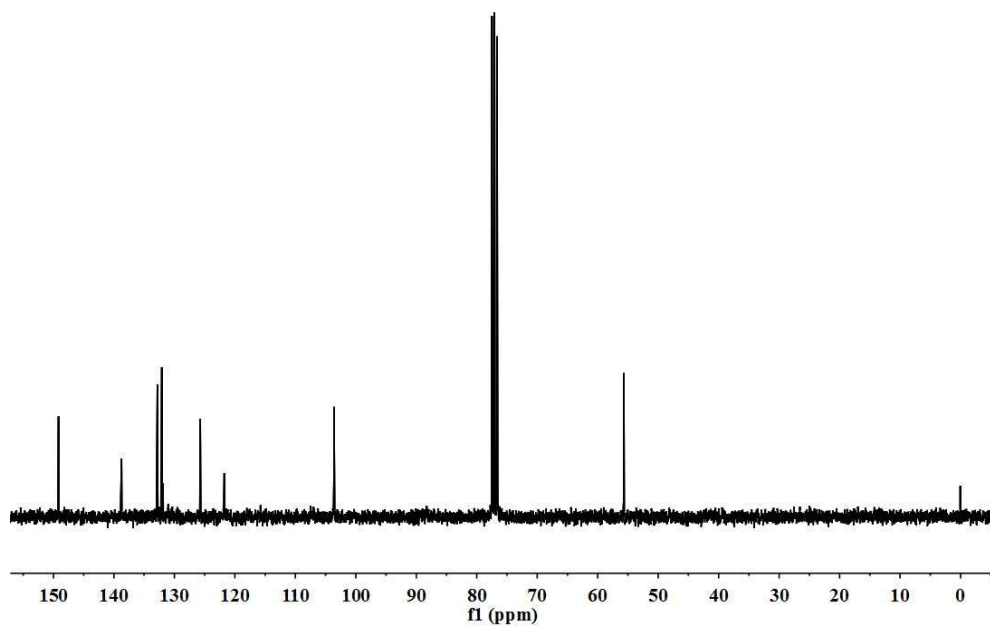


Figure S13. ¹³C NMR spectrum of compound 1.

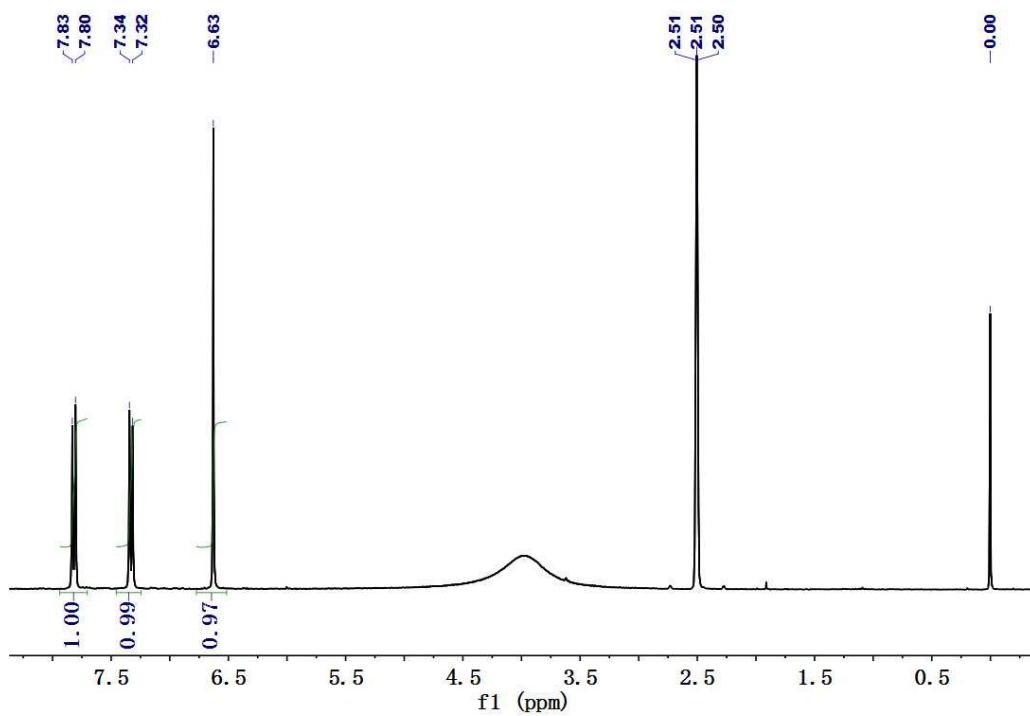


Figure S14. ¹H NMR spectrum of compound 2.

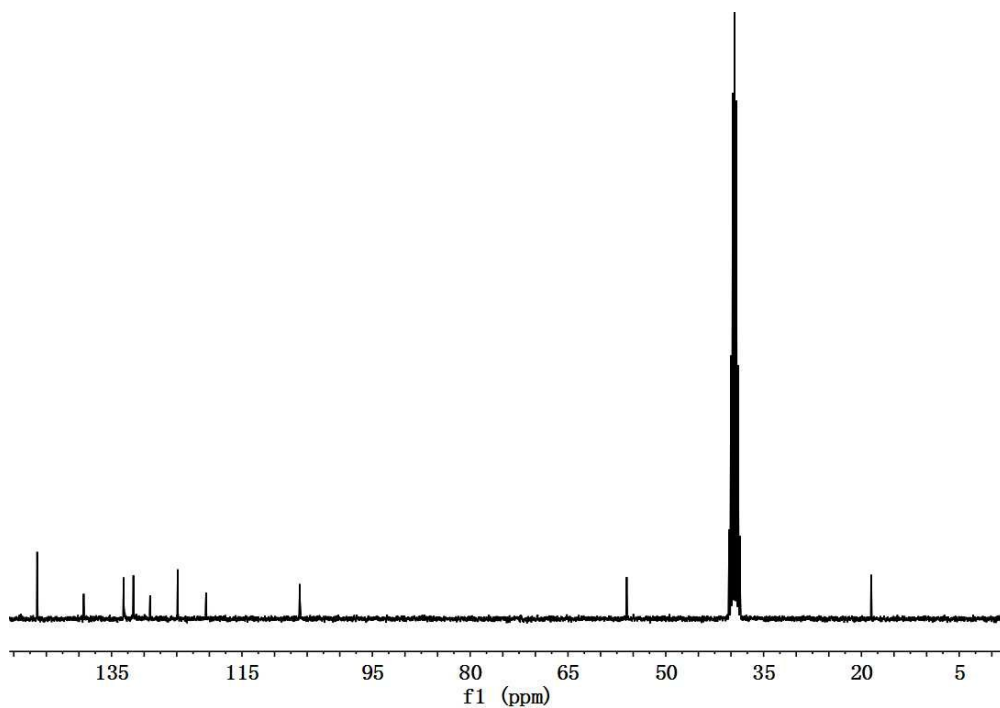


Figure S15. ¹³C NMR spectrum of compound 2.

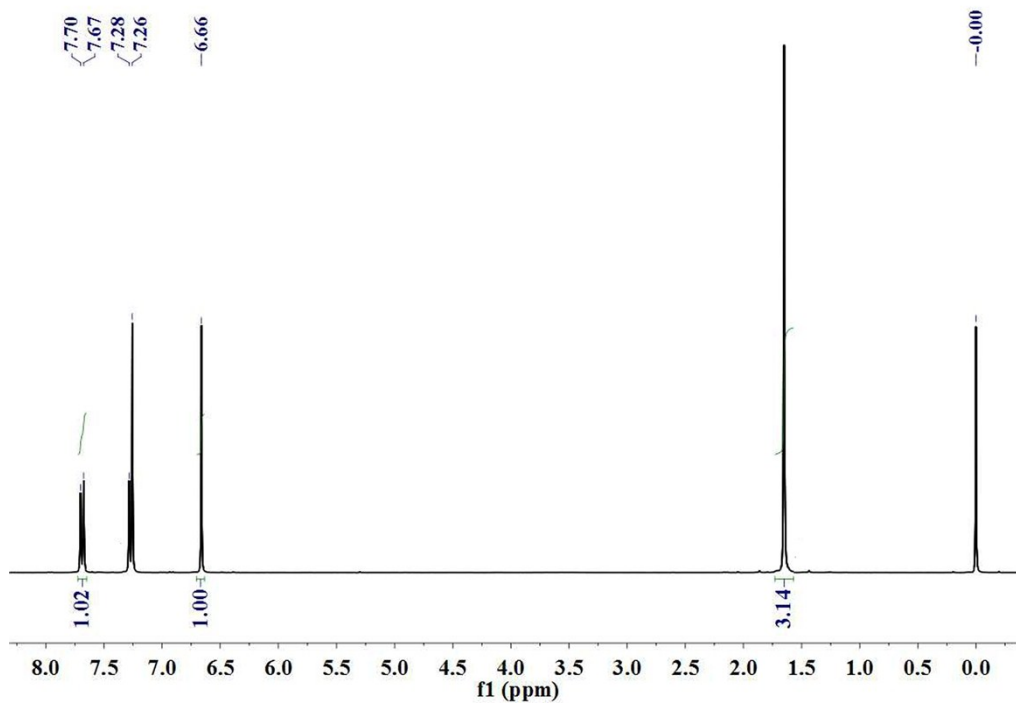


Figure S16. ¹H NMR spectrum of compound C2.

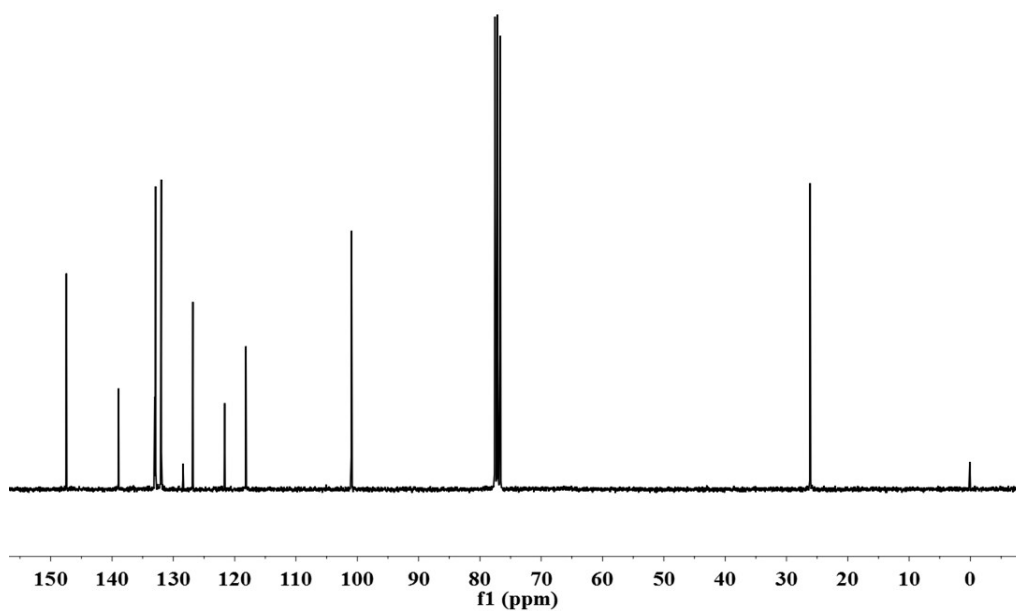


Figure S17. ¹³C NMR spectrum of compound C2.

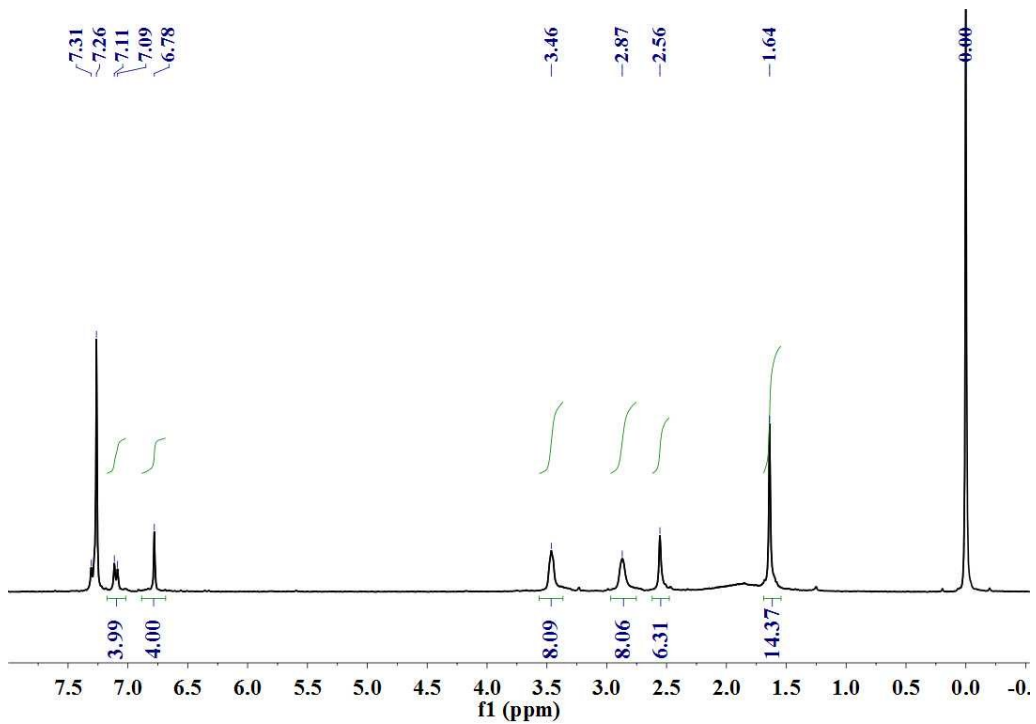


Figure S18. ¹H NMR spectrum of compound A2.

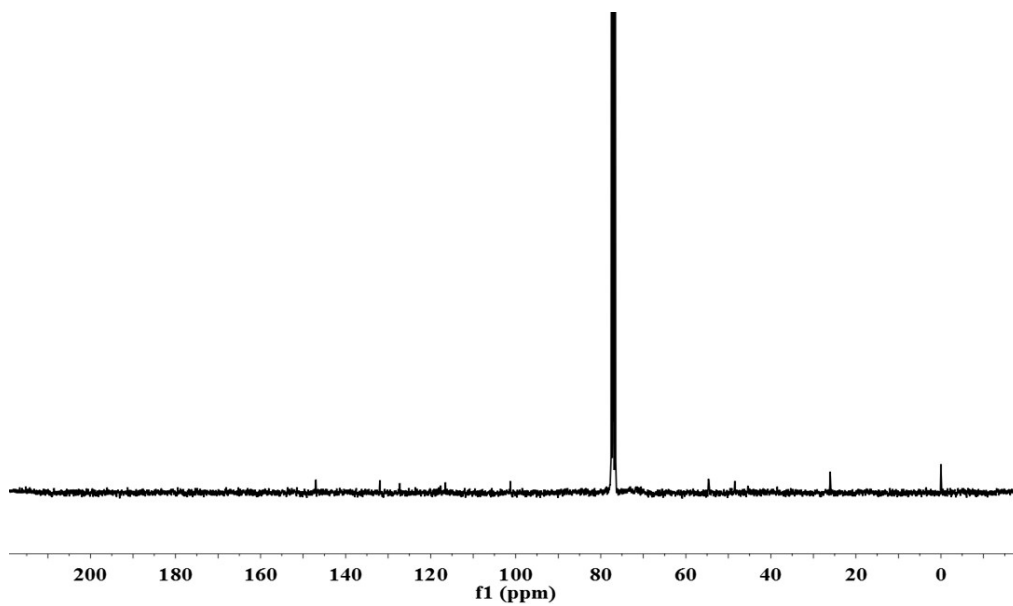


Figure S19. ¹³C NMR spectrum of compound A2.

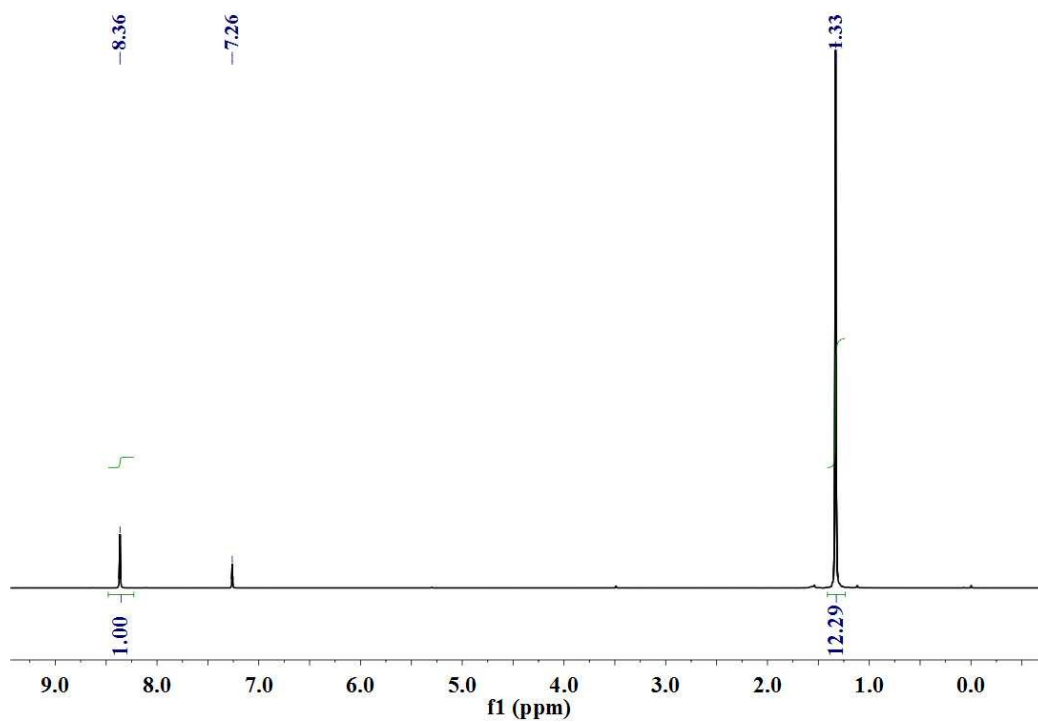


Figure S20. ^1H NMR spectrum of compound 3.

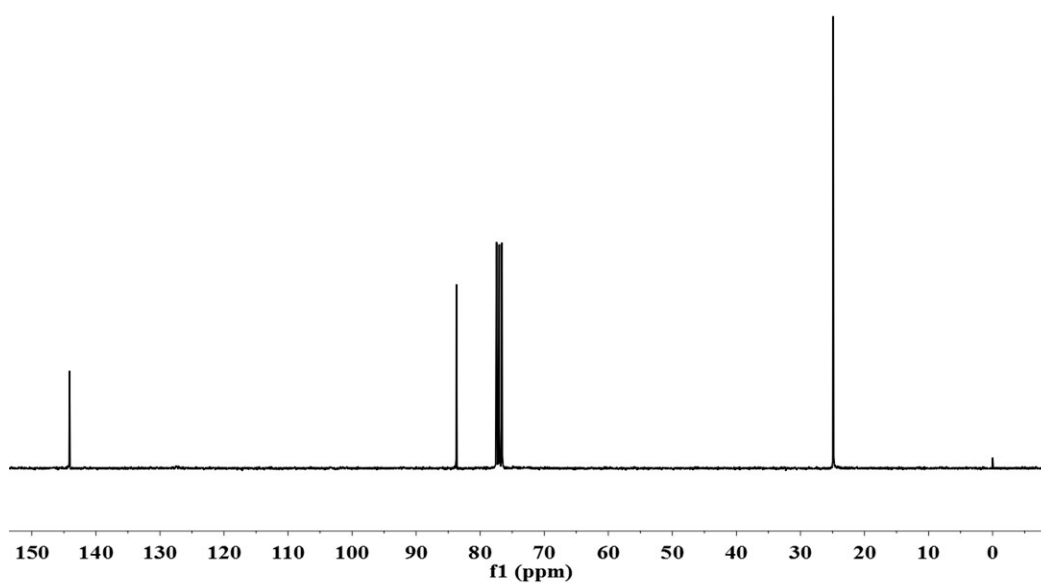


Figure S21. ^{13}C NMR spectrum of compound 3.

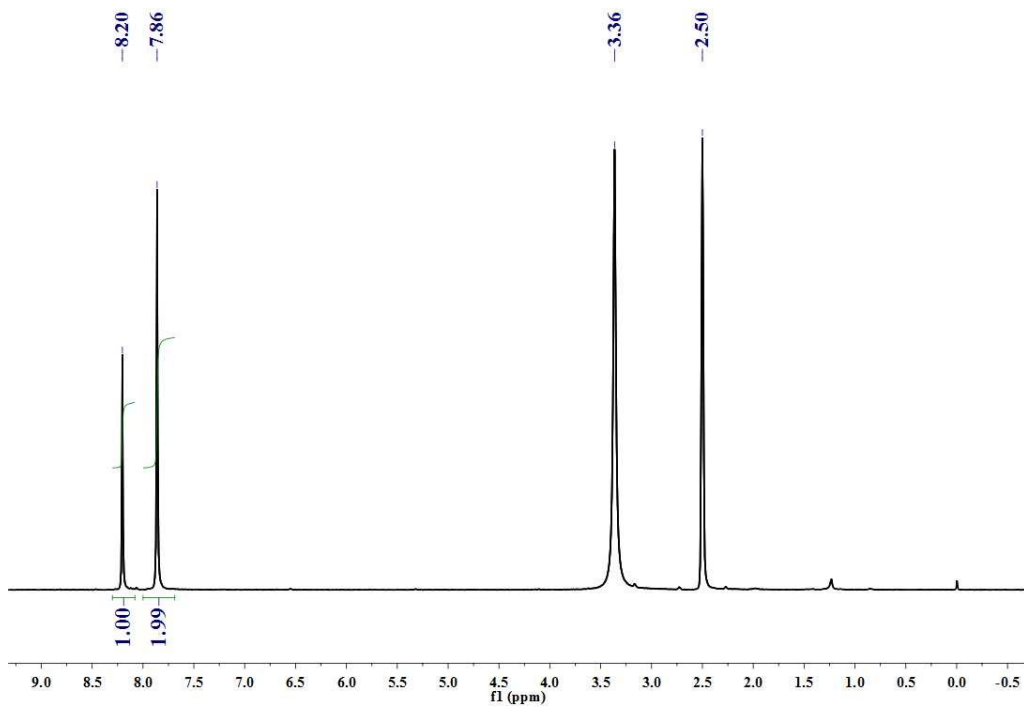


Figure S22. ^1H NMR spectrum of compound B3.

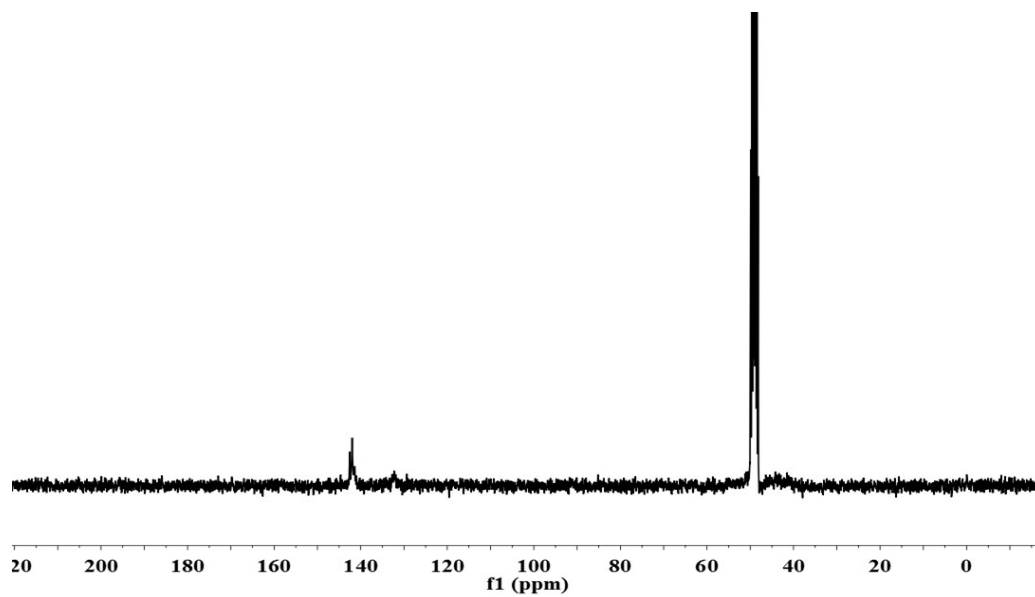


Figure S23. ^{13}C NMR spectrum of compound B3.

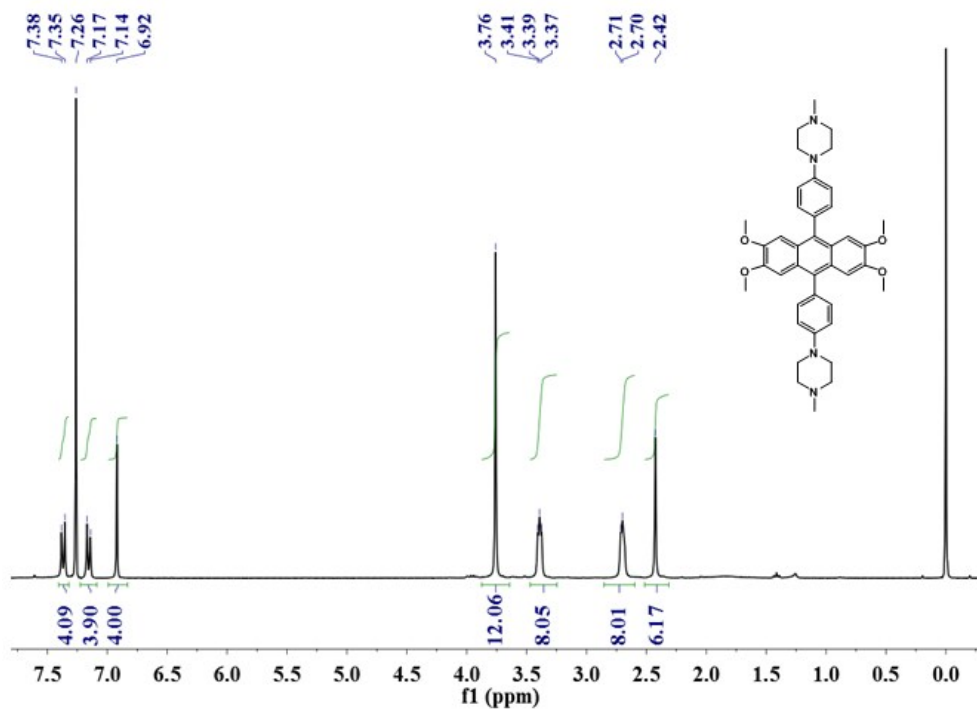


Figure S24. ^1H NMR spectrum of the compound 4.

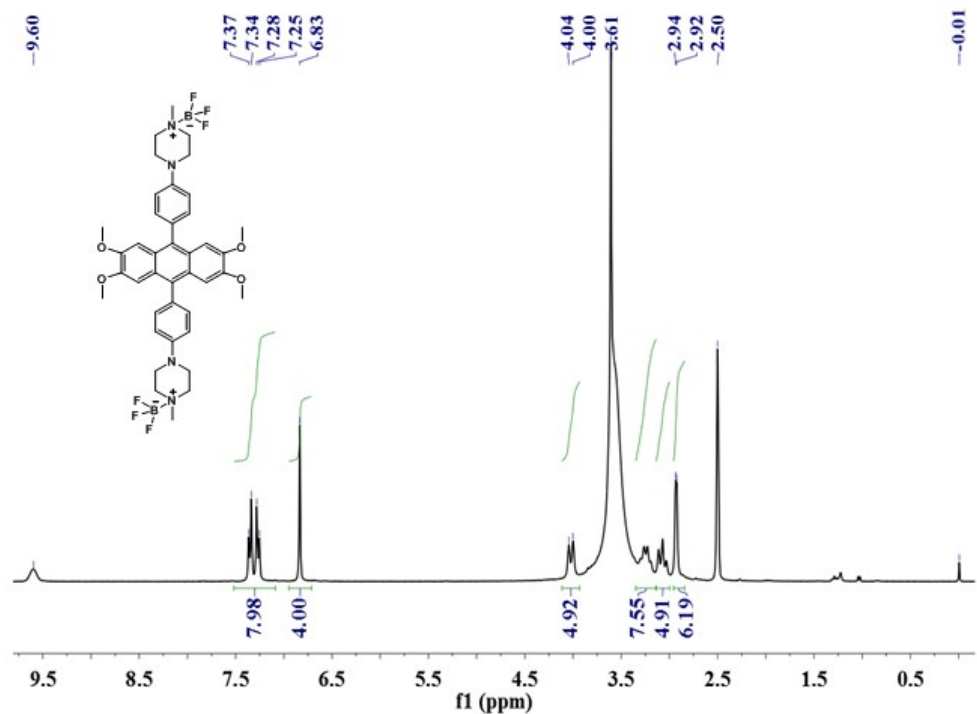


Figure S25. ^1H NMR spectrum of the model compound.

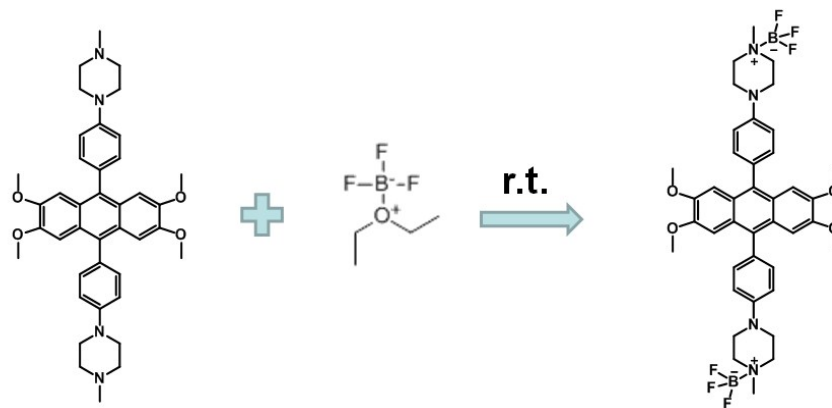


Figure S26. Synthetic route of the model compound.